0026-895X/05/6704-1247–1256$20.00
MOLECULAR PHARMACOLOGY
Copyright © 2005 The American Society for Pharmacology and Experimental Therapeutics
Mol Pharmacol 67:1247–1256, 2005

Vol. 67, No. 4
6130/1197422
Printed in U.S.A.

MOL PHARM

Arsenite Inhibition of CYP1A1 Induction by 2,3,7,8-Tetrachlorodibenzo-*p*-dioxin Is Independent of Cell Cycle Arrest

Jessica A. Bonzo, Shujuan Chen, Alema Galijatovic, and Robert H. Tukey

Laboratory of Environmental Toxicology, Departments of Pharmacology, Chemistry & Biochemistry, University of California, San Diego, La Jolla, California

Received August 12, 2004; accepted December 28, 2004

ABSTRACT

We show here that arsenite (As^{3+}) elicits multiple effects on gene control, such as the interruption of cell cycle control by initiating G_2/M arrest as well as inhibiting the aryl hydrocarbon (Ah) receptor-mediated 2,3,7,8-tetrachlorodibenzo-*p*-dioxin (TCDD)-inducible expression of CYP1A1. This raises the question as to whether As^{3+} is selectively inhibiting TCDD induction of CYP1A1 independent of cell cycle control. As^{3+} stimulated a concentration-dependent increase in G_2/M phase arrest that was detected at 12.5 μM As^{3+}. However, cotreatment of HepG2 cells with TCDD and concentrations of As^{3+} as low as 0.5 μM stimulated a pronounced decrease in the induction of CYP1A1-dependent ethoxyresorufin-*O*-deethylase activity and protein, indicating that the inhibition of CYP1A1 induction by As^{3+} was considerably more sensitive than As^{3+}-initiated cell cycle arrest. Low concentrations of As^{3+} also initiate a dose-dependent reduction in TCDD-induced mouse Cyp1a1 as well as human CYP1A1 in primary hepatocytes cultured from transgenic *CYP1A1N*$^{+/-}$ mice. Because primary hepatocytes in culture are quiescent, these results indicate that the actions of As^{3+} on TCDD-initiated induction of CYP1A1 are independent of cell cycle control. As^{3+} does not impact on Ah receptor function as evaluated by nuclear transport and binding to xenobiotic responsive element sequences, but it does reduce TCDD-induced CYP1A1 mRNA, a property that is concordant with RNA polymerase II association to the gene and the reduction in transcriptional heteronuclear RNA. We conclude from these studies that interruption of *CYP1A1*-induced transcription by As^{3+} is not dependent upon cell cycle arrest.

Inorganic arsenic (arsenite, As^{3+}) is an environmental contaminant released from a number of anthropogenic sources and results in As^{+3} sequestration in groundwater, which is often consumed as drinking water. Epidemiological studies indicate that chronic exposure is linked to vascular diseases associated with the cardiovascular and cerebrovascular systems, as well as the peripheral vasculature that leads to Blackfoot disease (Chiou et al., 1997; Lee et al., 2003; Tchounwou et al., 2003). In humans, As^{3+} exposure has also been thought to be a human carcinogen because epidemiological studies have linked As^{3+} exposure to skin, lung, liver, bladder, prostate, and kidney cancers (Smith et al., 1992; Tchounwou et al., 2003). However, exposure of laboratory animals to As^{3+} has failed to produce organ-specific cancers. This would indicate that cancers in humans linked to As^{3+} exposure may be associated with additional waterborne contaminants that work in concert to predispose humans to a carcinogenic episode. Although the relationship between As^{3+} exposure and other environmental toxicants associated with a carcinogenic episode is not known, it would seem that the actions of As^{3+} on cellular functions influence the biological actions of other environmental toxicants.

As^{3+} has been shown to alter cell cycle control, causing G_1 and/or G_2/M phase arrest with subsequent programmed cell death (Park et al., 2000; Yih and Lee, 2000). Evidence suggests that the phase arrest is induced by DNA damage. Telomere shortening and chromosome end-to-end fusions (Liu et al., 2003), oxidative DNA base modifications (Schwerdtle et al., 2003), and DNA strand breaks (Yih and Lee, 2000) indicate that small amounts of direct DNA damage can be caused by low concentrations of As^{3+}. If DNA damage is

This work was supported by Superfund Basic Research Program grant ES10337 from the U.S. Public Health Service.
Article, publication date, and citation information can be found at http://molpharm.aspetjournals.org.
doi:10.1124/mol.104.006130.

ABBREVIATIONS: Ah, aryl hydrocarbon; TCDD, 2,3,7,8-tetrachlorodibenzo-*p*-dioxin; Arnt, aryl hydrocarbon receptor nuclear translocator; PAH, polycyclic aromatic hydrocarbon; XRE, xenobiotic responsive element; DMSO, dimethyl sulfoxide; Pol, polymerase; PARP, poly(ADP-ribose) polymerase; DMEM, Dulbecco's modified Eagle's medium; MTT, 3-(4,5-dimethylthiazol-2-yl)-2,5-diphenyltetrazolium; DPBS, Dulbecco's phosphate-buffered saline; FACS, fluorescence-activated cell sorting; PI, propidium iodide; DTT, dithiothreitol; PMSF, phenylmethylsulfonyl fluoride; EROD, ethoxyresorufin-*O*-deethylase; hnRNA, heteronuclear RNA; PCR, polymerase chain reaction; GAPDH, glyceraldehyde-3-phosphate dehydrogenase; EMSA, electrophoretic mobility shift assay; RT-PCR, reverse transcriptase-polymerase chain reaction; AhR, aryl hydrocarbon receptor; P450, cytochrome P450.

MOLECULAR PHARMACOLOGY
aspet
Downloaded from molpharm.aspetjournals.org by guest on December 1, 2012

MOL PHARM

MOLECULAR PHARMACOLOGY

not repaired, p53 induces cell arrest, which eventually leads to apoptosis. It has been shown that p53 expression and ataxia telangiectasia-mutated-dependent activation associated with G_1 and G_2/M arrest and apoptosis is up-regulated upon As^{3+} treatment (Park et al., 2000; Yih and Lee, 2000; Filippova and Duerksen-Hughes, 2003). Thus, modulations in cell cycle control by As^{3+} exposure may impact on the expression of other cellular components.

The expression of CYP1A1 is dependent on the induction and activation of the aryl hydrocarbon (Ah) receptor. Cell cycle control has been shown to influence CYP1A1 expression through mechanisms involving the Ah receptor and other independent pathways. When murine hepa1c1c7 cells were treated with microtubule disrupters known to cause G_2/M phase arrest, induction patterns of Cyp1a1 after exposure to TCDD were dramatically reduced (Santini et al., 2001). In addition, this arrest seemed to not disrupt Ah receptor functionality. Analysis of Ah receptor and Arnt proteins revealed no decrease in protein levels, nor was nuclear translocation of the activated Ah receptor impaired in G_2/M-arrested cells. Further implication that cell cycle control has an effect on CYP1A1 expression comes from data demonstrating that pRb binds to the Ah receptor and is necessary for maximal CYP1A1 induction by TCDD in G_1 phase (Elferink et al., 2001).

Although As^{3+} can initiate cell cycle arrest, the levels of polycyclic aromatic hydrocarbon (PAH)-induced CYP1A1 are also inhibited when cells are exposed to As^{3+} (Jacobs et al., 1999; Vernhet et al., 2003). Because the Ah receptor is activated in response to PAHs leading to transcriptional activation of *CYP1A1*, it has been suggested that As^{3+} mediates the down-regulation of CYP1A1 through modulation of Ah receptor function. Transcriptional assays using reporter genes containing repeats of the xenobiotic responsive element (XRE) have demonstrated slight inhibition of transcriptional activity, suggesting that As^{3+} inhibits CYP1A1 induction through a transcriptional-based mechanism (Vernhet et al., 2003). However, the cellular mechanism underlying inhibition of CYP1A1 induction by As^{3+} remains largely unknown.

In this study, we have examined the effects of As^{3+} on Ah receptor control and the impact on TCDD-induced CYP1A1 expression. Given the known effects of As^{3+} on cell cycle control and apoptosis, the role of As^{3+}-induced G_2/M arrest on TCDD-initiated induction of CYP1A1 in HepG2 cells was investigated. Using a range of As^{3+} concentrations from subcytotoxic to levels that cause cellular arrest and apoptosis, we show that inhibition of CYP1A1 induction occurs at concentrations of As^{3+} well below those that initiate cell cycle arrest and apoptosis. The effects of As^{3+} on human *CYP1A1* gene expression in primary hepatocytes from transgenic mice (Galijatovic et al., 2004) coupled with analysis of polymerase II recruitment lead us to conclude that As^{3+} inhibits CYP1A1 expression by modifying transcription independent of cell cycle control.

Materials and Methods

Materials. TCDD was purchased from Wellington Laboratories Inc. (Guelph, ON, Canada) and dissolved in DMSO. Sodium arsenite and the horseradish peroxidase-conjugated secondary antibody were purchased from Sigma-Aldrich (St. Louis, MO). A mouse anti-human PARP-1 antibody was purchased from BD Biosciences PharMingen (San Diego, CA), and the mouse anti-human β-actin and anti-Pol II (sc-5943) were purchased from Santa Cruz Biotechnology, Inc. (Santa Cruz, CA). Rabbit anti-human CYP1A1 was a generous gift from Dr. Fred Guengerich (Vanderbilt University, Nashville, TN). The anti-human Ah receptor and anti-human Arnt antibodies were a generous gift from Dr. Christopher Bradfield (McArdle Laboratory for Cancer Research, University of Wisconsin, Madison, WI) and the anti-human UGT antibody was a generous gift from Dr. Wilbert H. Peters (St. Radboud University Hospital, Nijmegen, The Netherlands). All other chemicals and reagents were obtained through standard suppliers.

Cell Culture. The human hepatocarcinoma cell line HepG2 (American Type Culture Collection, Manassas, VA) and mouse liver hepatoma hepa1c1c7 cells (a generous gift of Dr. James Whitlock, Stanford University, Stanford, CA) were cultured in DMEM supplemented with 10% fetal bovine serum. TV101L cells were derived from HepG2 cells that stably express a *CYP1A1*-luciferase reporter gene (Postlind et al., 1993). TV101L cells were cultured under the same conditions as described above, except G418 (Geneticin; Invitrogen, Carlsbad, CA) was added to 0.8 mg/ml.

Primary hepatocytes were isolated from 8- to 12-week-old *CYP1A1N*$^{+/-}$ mice (Galijatovic et al., 2004). Mice were anesthetized by isoflurane inhalation. The portal vein was cannulated, and the anterior vena cava was sectioned to allow flow-through from the liver. Perfusion of the liver was started with Hanks' balanced salt solution (no Ca^{2+} or Mg^{2+}) containing 0.5 mM EGTA and 10 mM HEPES, pH 7.4, at a rate of 4 ml/min and continued for 4 min. The perfusate was then changed to Hanks' balanced salt solution (with Ca^{2+} and Mg^{2+}) containing 10 mM HEPES, pH 7.4, and 0.2 mg/ml collagenase. The liver was gently teased apart while in a solution of DMEM containing 10% fetal bovine serum supplemented with penicillin/streptomycin. The cells were filtered through a 70-μm cell strainer and washed twice by centrifugation at 50*g* for 5 min. The hepatocytes were cultured into six-well collagen-coated tissue culture plates (BD BioCoat; BD Biosciences Discovery Labware, Bedford, MA). Four hours after plating, the medium was replaced. Primary hepatocytes were then treated 48 h after seeding and collected at the appropriate times after treatment.

Cell Viability Assay (MTT Assay). Cell viability was measured by MTT as described previously (Mosmann, 1983). After treatment with various chemicals for 18 h, culture medium was replaced with serum-free medium containing 0.5 mg/ml MTT, and cultures were incubated for an additional 3 h. Assay medium was removed, and 1 ml of isopropanol with 0.04% HCl was added. Absorbance values were determined at 570 and 630 nm. Results are displayed as percentage of viable cells compared to TCDD-treated cells.

Cell Cycle Analysis. Approximately 1×10^6 HepG2 cells were exposed to TCDD and As^{3+} for 18 h, and the cells were collected by trypsinization and pelleted at 1000*g* for 5 min. Cells were washed twice with 1× DPBS and resuspended in 50 μl of 1× DPBS. Cells were fixed by the slow addition of 70% ethanol with constant vortexing to a volume of 5 ml. The cells were pelleted and resuspended in 800 μl of 1× DPBS containing 3% fetal bovine serum. Then, 100 μl of PI solution (final concentration 50 μg/ml PI) and 100 μl of boiled RNase A (final concentration 1 mg/ml) were added and incubated at 37°C for 30 min. Approximately 1×10^4 cells were acquired on a FACSCalibur flow cytometer and analyzed using the CELLQuest software.

Preparation of Cellular and Microsomal Protein. Total cellular protein was obtained by lysing cells directly on the tissue culture plates in 25 mM HEPES, pH 7.5, 0.3 M NaCl, 1.5 mM $MgCl_2$, 0.2 mM EDTA, 0.1% Triton X-100, 20 mM α-glycerophosphate, 0.5 mM DTT, 1 mM sodium orthovanadate, 0.1 μM okadaic acid, and 1 mM PMSF. The solubilized cell lysate was collected and centrifuged at 10,000*g*, and the supernatant was collected.

Microsomal protein was obtained by scraping cells from the tissue culture plates in a suspension of 10 mM KH_2PO_4, 0.15 M KCl, 2 mM PMSF, 2 mg/ml aprotinin, 0.2 mg/ml benzamidine, 0.5 mg/ml leu-

Downloaded from molpharm.aspetjournals.org by guest on December 1, 2012

MOL PHARM

MOLECULAR PHARMACOLOGY

peptin, and 1 μg/ml pepstatin. The cells were disrupted on ice by ultrasonic disruption using five repetitive 5-s bursts, followed by centrifugation at 10,000*g*. Supernatants were collected and centrifuged at 105,000*g* for 1 h in a Beckman TL100 tabletop ultracentrifuge. Microsomal pellet was resuspended in 100 μl of the phosphate buffer and stored at –70°C. All protein concentrations were determined by Bio-Rad analysis according to the manufacturer's instructions.

Western Blot Analysis. Western blots for detection of PARP-1 were performed using NuPAGE Bis-Tris gel electrophoresis units as outlined by the manufacturer (Invitrogen). A 20-μg aliquot of total cellular protein was heated for 10 min in loading buffer and resolved on a 10% Bis-Tris gel under reducing conditions, and protein was transferred to a nitrocellulose membrane using a semi-dry transfer system (Novex; Invitrogen). The membrane was blocked with 5% nonfat dry milk in Tris-buffered saline (0.01 M Tris, pH 8.0, 0.150 M NaCl, and 0.05% Tween 20) overnight at 4°C. This was followed by incubation with an anti-human/mouse PARP-1 primary antibody in Tris-buffered saline for 1 h at room temperature. Membranes were then washed and incubated for 1 h with horseradish peroxidase-conjugated secondary antibody at room temperature. The conjugated horseradish peroxidase was detected using ECL Plus Western blotting detection system (Amersham Biosciences Inc., Piscataway, NJ), and blots were exposed to X-ray film.

For detection of microsomal CYP1A1, 10 μg of microsomal protein was boiled in nonreducing loading buffer and added to Novex 10% Tris-glycine gels (Invitrogen), and electrophoresis carried out according to manufacturer's instructions. Membranes were then prepared as described above with the exception of the use of rabbit anti-human CYP1A1 primary antibody. For detection of CYP1A1 from primary hepatocytes, 20 μg of total cellular protein was used, and blots performed as described for microsomal CYP1A1.

Detection of Ethoxyresorufin *O*-deethylase Activity. EROD measurement was performed as described previously (Ciolino et al., 1998). Approximately 2.5×10^5 cells/well were plated in six-well plates. Cells were exposed to TCDD and As^{3+} for 18 h, and the media were removed and replaced with DMEM containing 10% fetal bovine serum, 1.5 mM salicylamide, and 2.5 μM 7-ethoxyresorufin. After incubation for 30 min at 37°C, the media were removed, and fluorescence was measured with 530-nm excitation and 590-nm emission on a FluoroMax-2 (HORIBA Jobin Yvon SPEX Instruments, Inc., Edison, NJ). Resorufin standard curves were used to convert fluorescence to picomoles of resorufin formed. Results were normalized to reaction time and cellular protein.

For determination of microsomal EROD activity, microsomes were collected and resuspended in 50 mM Tris-HCl, pH 7.5, 20% glycerol (v/v), and 1 mM DTT. Reactions contained 20 μg of protein and 8 μM 7-ethoxyresorufin and were initiated by the addition of 1 mM NADPH. After incubation for 30 min at 37°C, each reaction was stopped with the addition of chilled methanol. Fluorescence was detected as described above.

RNA Analysis for *CYP1A1* Expression. Total RNA was extracted from cells using TRIzol (Invitrogen) according to manufacturer's protocol and resuspended in diethyl pyrocarbonate-treated water. Each preparation of RNA was treated with DNase using a DNA-free kit (Ambion, Austin, TX). Levels of CYP1A1 mRNA and heteronuclear RNA (hnRNA) were quantitated by real-time PCR. After oligo(dt)-primed reverse transcription using 2 μg of total RNA with Omniscript RT (QIAGEN, Valencia, CA), the cDNA was amplified with forward (5′-TAG-ACA-CTG-ATC-TGG-CTG-CAG-3′) and reverse (5′-GGG-AAG-GCT-CCA-TCA-GCA-TC-3′) human CYP1A1 mRNA primers. Primers for human CYP1A1 hnRNA were published previously (Hestermann and Brown, 2003). For quantitation of human GAPDH, the forward (5′-GCT-GAG-ACA-CCA-TGG-GGA-AG-3′, bases 93–113) and reverse (5′-CTT-CCC-GTT-CTC-AGC-CTT-GA-3′, bases 282–301) primers were identified from the cDNA sequence (GenBank accession no. AF261085). Each RNA was amplified in a 50-μl PCR reaction that contained 25 μl of QuantiTect SYBR Green PCR Master Mix (QIAGEN), 100 nM each of forward and reverse primers, and 2 μl of cDNA. The initial activation was proceeded at 95°C for 10 min followed by 40 cycles of amplification: 95°C for 30 s, 60°C for 1 min, and 72°C for 45 s. Amplification was followed by DNA melt at 95°C for 1 min and a 41-cycle dissociation curve starting at 55°C and ramping 1°C every 30 s. The MX4000 Multiplex QPCR (Stratagene, La Jolla, CA) was programmed to take three fluorescence data points at the endpoint of each annealing plateau. All PCR reactions were performed in triplicates. CYP1A1 C(t) values were normalized to GAPDH C(t) values [ΔC(t)]. CYP1A1 cDNA and hnRNA was expressed as induction fold of vehicle-treated cells using the equation ratio $= 2^{-(\Delta CtSample\ -\ \Delta CtVehicle)}$ (Pfaffl, 2001). TCDD-treated samples were set to maximal induction, and all other treatments are expressed as a percentage of TCDD induction of CYP1A1 mRNA.

Nuclear and Cytosolic Protein Preparation. Nuclear protein was prepared as described previously (Chen and Tukey, 1996), and all procedures were performed at 4°C. After treatment, the tissue culture plates were washed twice with ice-cold 10 mM HEPES. Cells were collected by scraping into MDH buffer (3 mM $MgCl_2$, 25 mM HEPES, 1 mM DTT, 0.2 mM PMSF, 10 μg/ml aprotinin, and 10 μg/ml leupeptin) and homogenized with a Dounce homogenizer. The homogenate was centrifuged at 2500*g* for 5 min, and the resulting nuclear pellet was resuspended and washed three times with MDHK buffer (3 mM $MgCl_2$, 25 mM HEPES, 0.1 M KCl, 1 mM DTT, 0.2 mM PMSF, 10 μg/ml aprotinin, and 10 μg/ml leupeptin). The nuclear fraction was resuspended in 100 μl of HDK buffer (25 mM HEPES, 0.4 M KCl, 1 mM DTT, 0.2 mM PMSF, 10 μg/ml aprotinin, and 10 μg/ml leupeptin), incubated for 30 min on ice, and centrifuged at 16,000*g* for 15 min. The resulting supernatant was transferred to ultracentrifuge tubes, adjusted to a final concentration of 10% glycerol, and centrifuged at 105,000*g* for 1 h. Each nuclear protein aliquot was stored at –70°C.

Cytosols were prepared from untreated hepa1c1c7 cells as described previously (Chen and Tukey, 1996). In brief, cells washed in HEPES were collected by scraping in HED buffer (25 mM HEPES, pH 7.5, 1 mM EDTA, and 1 mM DTT). The cells were homogenized with a Dounce homogenizer and then diluted 1:1 with HED2G (25 mM HEPES, pH 7.5, 1 mM EDTA, 1 mM DTT, and 20% glycerol). The homogenate was centrifuged at 105,000*g* for 1 h, and the supernatant was collected. Cytosolic Ah receptor was activated by incubation of cytosol with 20 nM TCDD for 24 h at 4°C.

Electrophoretic Mobility Shift Assay (EMSA). As described previously (Yueh et al., 2003), nuclear or cytosolic extracts were incubated on ice for 15 min with 2.2 μg of poly(dI-dC) and 1 μg of salmon sperm DNA in HEDG buffer (25 mM HEPES, pH 7.4, 1.5 mM EDTA, 10% glycerol, and 1 mM DTT). A ^{32}P-labeled XRE oligonucleotide probe (5×10^5 cpm) was added, and the reaction was incubated at room temperature for 15 min. Loading dye was added, and the proteins were resolved on a 6% nondenaturing polyacrylamide gel. Radioactively bound proteins were visualized by exposure to a PhosphorImager plate and scanning with a Molecular Dynamics Storm 840 scanner (Amersham Biosciences).

Luciferase Activity Assay. Luciferase assays were performed as described previously (Chen and Tukey, 1996). TV101L cells were treated and lysed on plates in lysis buffer (1% Triton, 25 mM tricine, pH 7.8, 15 mM $MgSO_4$, 4 mM EDTA, and 1 mM DTT). Cell lysates were collected by centrifugation at 10,000*g* in a microcentrifuge for 10 min at 4°C. Supernatant (10 μl) was mixed with 300 μl of reaction buffer (25 mM tricine, 15 mM $MgSO_4$, 4 mM EDTA, 15 mM KPO_4, pH 7.8, 1 mM DTT, and 2 mM ATP). Reactions were started by the addition of 100 μl of luciferin (0.3 mg/ml), and light output was measured for 10 s at 24°C using a Monolight 2001 luminometer (Analytical Luminescence Laboratory, Ann Arbor, MI). Results were normalized by Bradford protein assay and expressed as fold induction of vehicle control.

Chromatin Immunoprecipitation Assay. Method was based on those published previously (Hestermann and Brown, 2003; Wei

Downloaded from molpharm.aspetjournals.org by guest on December 1, 2012

MOL PHARM
MOLECULAR PHARMACOLOGY
aspet

et al., 2004). HepG2 cells were grown to confluence on 150-cm plates and then treated for 1 h with DMSO, TCDD, 0.5 μM As^{3+} + TCDD, or 5 μM As^{3+} + TCDD. Cells were cross-linked by addition of formaldehyde to 1% directly to culture media for 10 min. Cross-linking was stopped by the addition of 125 mM glycine, and cells were incubated at room temperature for 10 min with gentle rocking. Plates were washed with phosphate-buffered saline, and then cells were collected by scraping in ice-cold phosphate-buffered saline. Cellular pellet was lysed (1% SDS, 5 mM EDTA, 50 mM Tris, pH 8, and protease inhibitors) for 10 min on ice and then sonicated 3 × 15 s at 20 W in 1-min intervals. The sample was cleared of cellular debris by centrifugation at 16,000*g* for 10 min at 4°C. One hundred-microliter aliquots were diluted to 1 ml in dilution buffer (1% Triton, 2 mM EDTA, 20 mM Tris, pH 8, 150 mM NaCl, and protease inhibitors) and precleared for 1 h at 4°C with 50 μl of protein agarose A/G (Santa Cruz Biotechnology, Inc.) with 1 μg/μl salmon sperm DNA. Aliquots were removed at this time for use as input control and processed along with pull-down DNA at reversal of cross-linking step. Precleared supernatants were then incubated overnight at 4°C on a rotating platform with 1 μg of α-Pol II. Fifty microliters of protein agarose A/G plus salmon sperm DNA was added and incubated on rocking platform for 1 h at 4°C. Beads were pelleted and washed for 10 min each in the following buffers (buffer 1, 0.1% SDS, 2 mM EDTA, 20 mM Tris, and 150 mM NaCl; buffer 2, 0.1% SDS, 2 mM EDTA, 20 mM Tris, and 500 mM NaCl; and buffer 3, 1% LiCl, 1% Nonidet P-40, 1% deoxycholate, 1 mM EDTA, and 10 mM Tris). Pellets were washed twice in Tris/EDTA buffer and then eluted in 100 μl of 1% SDS, 0.1 M sodium bicarbonate, and 0.2 M NaCl at 65°C overnight. Eluates were digested with proteinase K at 45°C for 1 h and then purified using QIAGEN spin columns. DNA was quantitated using a spectrophotometer. Equal amounts of pulled-down DNA as well as input controls were used for each quantitative real-time PCR reaction. Amplification of the proximal promoter was achieved using primers that span a 250-base pair region that includes the transcription start site (forward 5′-AGA-AAG-GGC-AAG-CCA-GAA-GT-3′ and reverse 5′-TCC-AAT-CCC-AGA-GAG-ACC-AG-3′). Results are displayed as raw C(t) values and representative of three independent experiments.

Statistical Analysis. All experiments were performed in triplicate. Statistical analysis was performed where indicated using two-tailed *t* test assuming unequal variances. Differences were determined to be significant if $P \leq 0.05$.

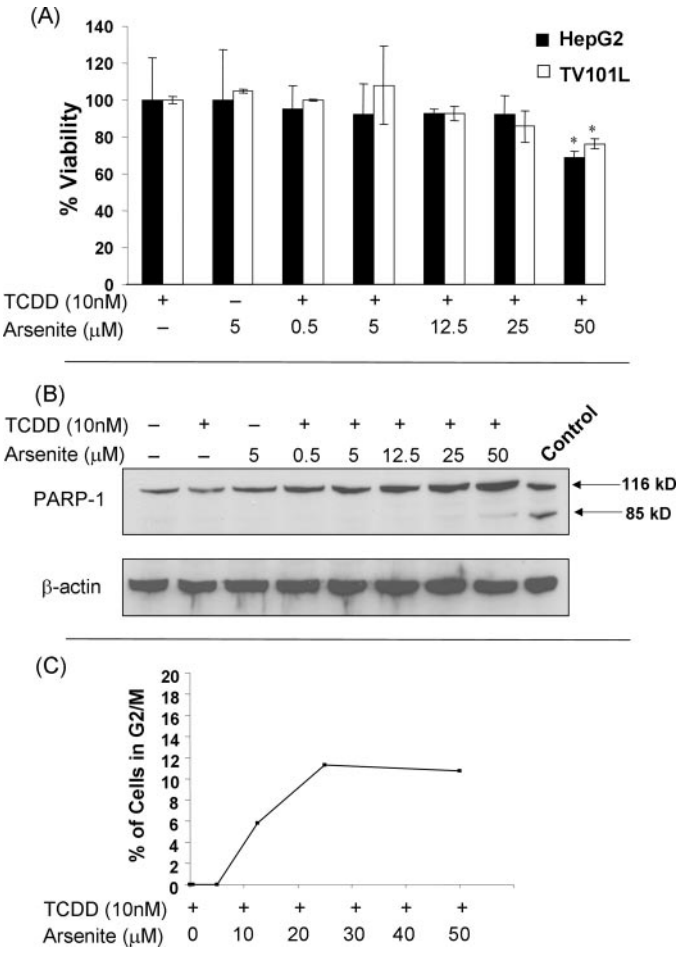

Fig. 1. Cell viability, apoptosis, and cell cycle arrest after As^{3+} exposure. A, HepG2 and TV101L cells were treated with 10 nM TCDD and indicated concentrations of As^{3+} for 18 h. Cell viability was measured using the MTT assay and expressed as percentage of viability compared with TCDD-treated cells. Experiments were performed in triplicate. Significant decrease from viability of TCDD-treated cells is indicated (*, $P \leq 0.05$). B, HepG2 cells were treated with 10 nM TCDD and indicated concentrations of As^{3+} for 18 h. Twenty micrograms of whole cell extract was used for Western blot analysis of PARP-1 cleavage. Intact PARP-1 (116 kDa) and cleaved PARP-1 (85 kDa) are indicated. Extracts from benzo[*a*]pyrene-*r*-7,*t*-8-dihydrodiol-*t*-9,10-epoxide-treated cells was used as a positive control for cleavage. Blots were rewashed and exposed to anti-β-actin for loading control. C, HepG2 cells were treated with 10 nM TCDD and various concentrations of As^{3+} for 18 h before fixation. Ten thousand PI-stained cells were acquired on a FACSCalibur flow cytometer, and the percentage of cells in G_2/M as a result of As^{3+} treatment is shown. Cells were treated with TCDD or TCDD and increasing As^{3+} concentrations. Data shown indicate the percentage of the total cells counted that were in G_2/M phase after As^{3+} treatment and are representative of three independent FACS analyses.

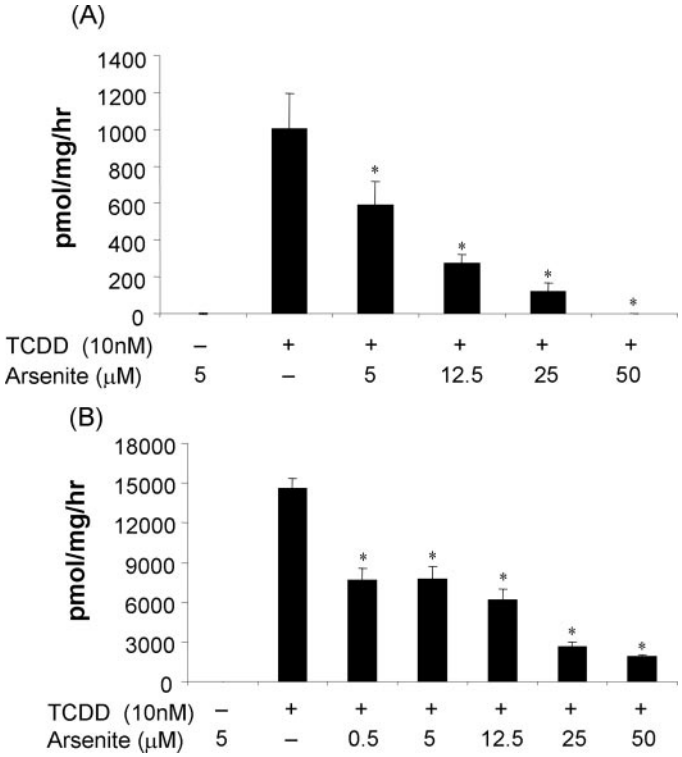

Fig. 2. EROD activity as a function of As^{3+} treatment. A, HepG2 cells were treated with 10 nM TCDD and increasing concentrations of As^{3+} for 18 h, and cellular EROD activity was measured as outlined under *Materials and Methods*. B, HepG2 cells were treated with 10 nM TCDD and increasing concentrations of As^{3+} for 18 h, and microsomes were collected. Microsomal EROD activity was determined using 20 μg of protein in reaction mixture as outlined under *Materials and Methods*. Significant decreases in EROD activity from TCDD treatment are indicated (*, $P \leq 0.05$).

Downloaded from molpharm.aspetjournals.org by guest on December 1, 2012

MOL PHARM
MOLECULAR PHARMACOLOGY
aspet

Results

Effect of As^{3+} on Apoptosis and Cell Cycle. As^{3+} has been shown to interrupt normal cell function by interfering with cell cycle control and by initiating apoptosis. To examine the impact of As^{3+} on HepG2 cells, we treated cells with a range of As^{3+} concentrations and measured cell viability by MTT analysis (Fig. 1A) and apoptosis by detecting caspases activated PARP-1 cleavage (Fig. 1B). Comparisons were made over a range of As^{3+} concentrations that also included cotreatment with 10 nM TCDD. At concentrations of As^{3+} ranging from 0.5 to 25 μM, no changes in cell viability or the initiation of apoptosis were noted. TCDD alone or in combination with As^{3+} at these concentrations did not affect cell function. However, cell viability was reduced 30% in HepG2 cells treated with 50 μM As^{3+}, which correlated with a mild increase in caspases activated PARP-1 cleavage. When cell cycle status was evaluated, As^{3+}-treated HepG2 cells revealed an increase in G_2/M cell cycle arrest at concentrations that exceeded 12.5 μM (Fig. 1C). Analysis of HepG2 cells treated with As^{3+} alone was consistent with the results shown in Fig. 1C, indicating that the increase in G_2/M arrest was attributed solely to the actions of As^{3+}.

As^{3+} Treatment Blocks TCDD Induction of CYP1A1. The cotreatment of HepG2 cells with As^{3+} and TCDD elicited significant inhibition of TCDD-dependent induction of EROD activity over a concentration range from 5 to 50 μM As^{3+} (Fig. 2A). An excellent correlation was observed when EROD activity was measured both in whole cells as well as in HepG2 cell microsomal preparations (Fig. 2B), indicating that the expression of CYP1A1 was dramatically impaired. This was confirmed by Western blot analysis of induced CYP1A1. The pattern of EROD activity correlated with a concentration-dependent reduction in CYP1A1 protein (Fig. 3A).

Quantitation of TCDD inducible CYP1A1 mRNA by real-time RT-PCR demonstrated that the levels of mRNA after TCDD and As^{3+} treatment were concordant with reductions seen in CYP1A1 by Western blot analysis. At 0.5 μM As^{3+}, a concentration that has no detectable effect on cell cycle control, CYP1A1 mRNA induction decreased by 61% of the levels observed with TCDD treatment alone (Fig. 3B). At 50 μM As^{3+} cotreatment, a 90% decrease in TCDD induction of CYP1A1 mRNA was observed.

The levels of As^{3+} needed to block induction of CYP1A1 were 10-fold lower than those shown to stimulate G_2/M arrest, indicating that those events associated with cell cycle control may have limited impact on induction of CYP1A1. However, we cannot exclude the possibility that analysis of cell cycle control in the presence of lower concentrations of As^{3+} may lie outside the detection limits of flow cytometry. To compensate for this possibility, an experiment was conducted using cultured mouse liver hepatocytes isolated from transgenic *CYP1A1N*$^{+/-}$ mice (Gali-

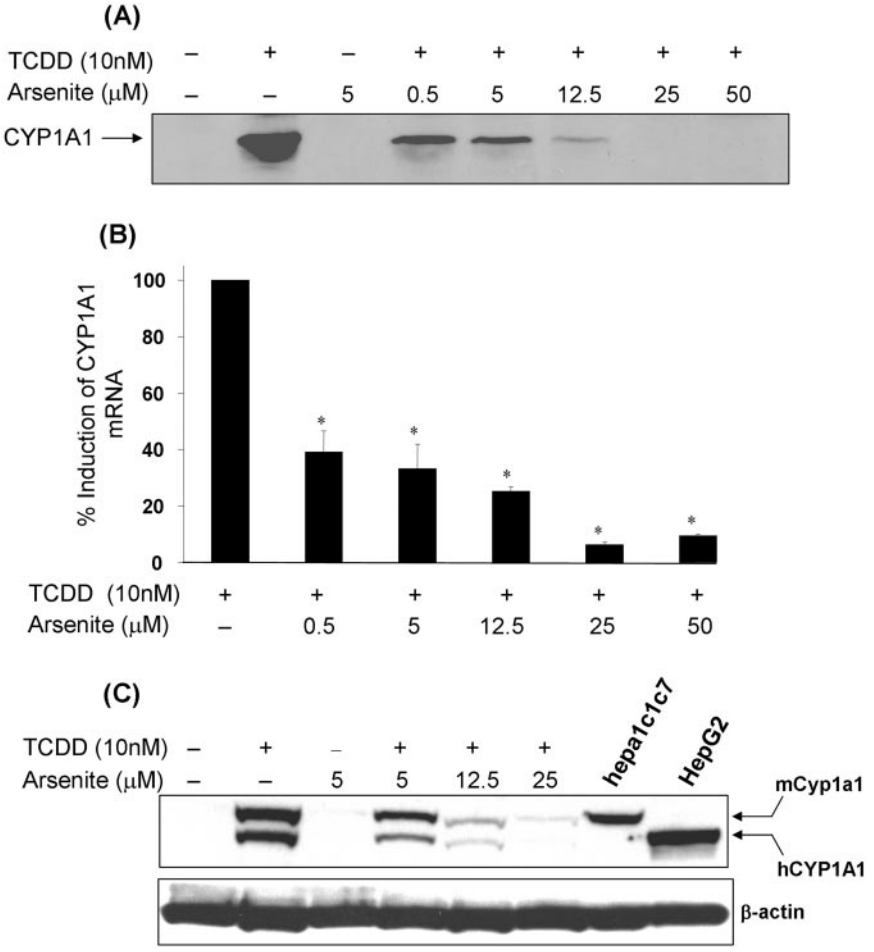

Fig. 3. CYP1A1 protein and mRNA expression decreases with As^{3+} treatment. A, HepG2 cells were treated with 10 nM TCDD and various concentrations of As^{3+} for 18 h at which time microsomes were collected. Ten micrograms of microsomes were used for Western blot analysis. B, real-time RT-PCR results were normalized to GAPDH and expressed as percentage of induction of TCDD-treated cells. Significant decreases in mRNA expression from TCDD treatment are indicated (*, $P \leq 0.05$). C, primary hepatocytes were isolated from *CYP1A1N*$^{+/-}$ transgenic mice and exposed in culture to TCDD and various As^{3+} concentrations. Whole cell lysates were collected and 20 μg of protein used for Western blot detection using the human CYP1A1 antibody that is cross-reactive with mouse Cyp1a1. Whole cell extracts from TCDD-treated hepa1c1c7 cells were used as a positive control for mouse Cyp1a1 and TCDD-treated HepG2 whole cell extracts were used as a human CYP1A1 positive control.

Downloaded from molpharm.aspetjournals.org by guest on December 1, 2012

MOL PHARM

MOLECULAR PHARMACOLOGY

jatovic et al., 2004). When primary hepatocytes are placed in culture, they become quiescent so cell cycle control cannot be credited with alterations in gene expression patterns. Because *CYP1A1N*$^{+/-}$ mice express the full-length human *CYP1A1* gene, induction of mouse Cyp1a1 and human CYP1A1 can be evaluated simultaneously. As shown in Fig. 3C, treatment of hepatocytes with TCDD resulted in a marked induction of Cyp1a1 and CYP1A1. As^{3+} cotreatment inhibited in a dose-dependent manner TCDD induction of both mouse Cyp1a1 and human CYP1A1. The inability of lower concentrations of As^{3+} to inhibit cell cycle control in HepG2 cells combined with the observations that As^{3+} can inhibit induction of CYP1A1 in *CYP1A1N*$^{+/-}$-derived primary hepatoctyes indicates that the cellular mechanisms initiated by As^{3+} on cell cycle control do not influence those events that lead to inhibition of CYP1A1 induction by Ah receptor ligands.

The Actions of As^{3+} on TCDD-Induced Transcriptional Control of CYP1A1. The reduction in TCDD enhancement of CYP1A1 by As^{3+} might indicate that cellular control of the Ah receptor is a potential target for the actions of As^{3+}. When cytosolic preparations from hepa1c1c7 cells are incubated with TCDD, the Ah receptor forms a complex with Arnt, generating a transcriptional complex capable of binding to DNA. Ah receptor activation can be demonstrated by receptor binding to XRE sequences, as demonstrated by EMSA. In Fig. 4, the addition of TCDD to hepa1c1c7 cytosol leads to the identification of an Ah receptor (AhR)/XRE complex (lane 5). The binding of activated Ah receptor was shown to be specific by the reduction in labeled protein/DNA interactions when the reaction was incubated with excess of unlabeled XRE oligonucleotide (Fig. 4, lane 6). Incubation with an inhibitor of Ah receptor ligand binding (α-naphthoflavone) also demonstrates a specific reduction in binding (Fig. 4, lane 7). However, when increasing concentrations of As^{3+} were included in the binding reaction, no inhibition of Ah receptor binding to the XRE sequences was noted.

To examine the impact of As^{3+} on TCDD-induced nuclear accumulation of the Ah receptor, HepG2 cells were treated with TCDD or cotreated with TCDD and As^{3+} for 18 h, and nuclear accumulation of the Ah receptor was determined by EMSA. The treatment of HepG2 cells with 10 nM TCDD leads to the accumulation of nuclear Ah receptor, which can be specifically identified by disruption of binding to XRE sequences when antibodies to the Ah receptor and Arnt protein are included in the binding reaction (Fig. 5B). When HepG2 cells are cotreated with TCDD and varying concentrations of As^{3+} for 18 h, no disruption in the accumulation of nuclear Ah receptor complex is observed (Fig. 5A).

To examine directly the impact of As^{3+} on TCDD-initiated *CYP1A1* transcription, TV101L cells that express the human *CYP1A1* promoter upstream of the firefly luciferase reporter gene were used. Treatment with TCDD induced luciferase activity 50-fold over that of untreated cells (Fig. 6A). When TV101L cells were cotreated with 10 nM TCDD and varying concentrations of As^{3+} for 18 h, As^{3+} had negligible effects on TCDD-initiated induction of *CYP1A1*-luciferase activity.

Because activation of the Ah receptor and the initiation of transcription are not influenced by As^{3+} exposure, we elected to determine whether the rate of *CYP1A1* transcription was altered by measuring the levels of CYP1A1 hnRNA RNA. Quantization of hnRNA is a measurement of the abundance of nuclear transcripts and reflects the rate

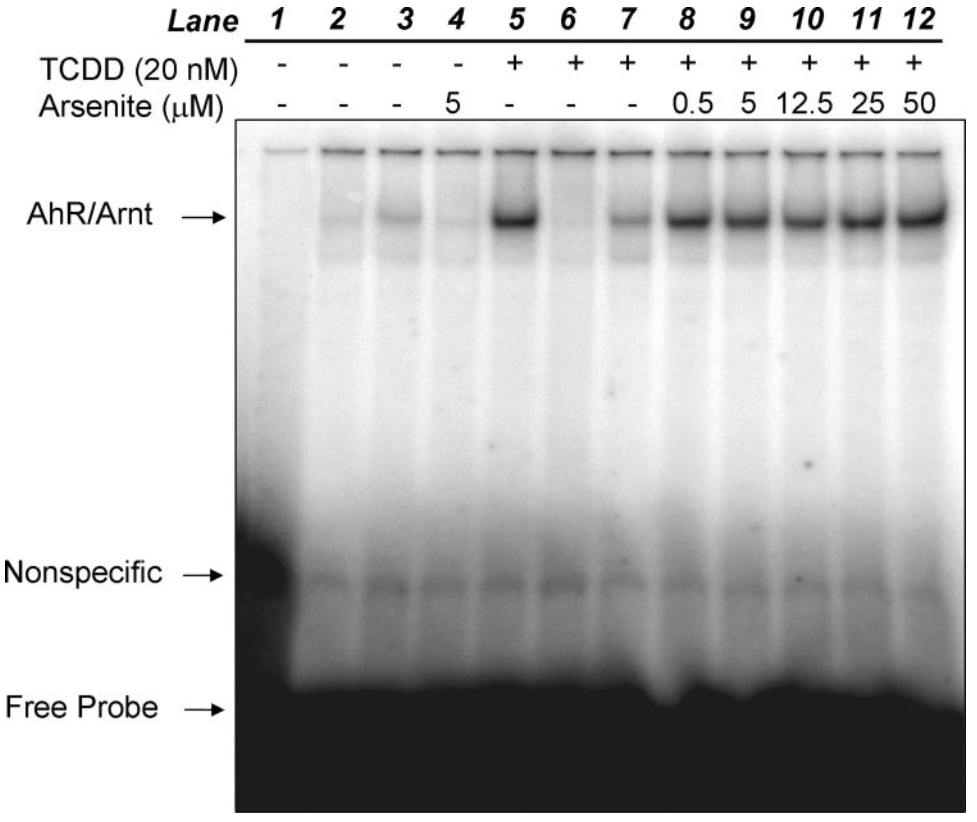

Fig. 4. Activation of Ah receptor is unaffected by the presence of As^{3+}. Cytosolic extracts (50 μg) from untreated hepa1c1c7 cells were incubated with 20 nM TCDD and indicated As^{3+} concentrations for 20 h at 4°C. Gel shift was performed as described in text. Control reactions are as follows: free probe (lane 1), water (lane 2), DMSO (lane 3), 5 μM As^{3+} (lane 4), 20 nM TCDD (lane 5), 20 nM TCDD and 200× unlabeled XRE (lane 6), and 20 nM TCDD + 1 μM β-naphthoflavone (lane 7). Coincubation of TCDD and As^{3+} is indicated (lanes 8–12). Activated AhR/Arnt heterodimer is indicated. Gel shift is representative of three independent experiments.

Downloaded from molpharm.aspetjournals.org by guest on December 1, 2012

of RNA synthesis at any steady-state level. In this experiment, cells were treated for 1 h with either TCDD or cotreated with TCDD and As^{3+}, and the nuclear CYP1A1 RNA quantitated by real-time RT-PCR using primers that amplify the exon-intron boundary of exon 1 (Hestermann and Brown, 2003). Treatment of HepG2 cells with TCDD induced CYP1A1 hnRNA after 1-h treatment (Fig. 6B). When cells were cotreated with TCDD at either 0.1 or 0.5 μM As^{3+}, reduction in the abundance of the hnRNA transcript was noted. The low concentrations of As^{3+} were comparable with those that inhibited the induction of mRNA and protein. Thus, As^{3+} seems to interfere with the transcriptional processes that promote induction of CYP1A1.

Confirmation of the inhibition of transcription on the *CYP1A1* promoter was obtained by the chromatin immunoprecipitation assay. HepG2 cells were treated for 1 h with TCDD or TCDD with either 0.5 μM As^{3+} or 5 μM As^{3+}. The pull down was performed with an antibody specific to RNA polymerase II (Pol II), and real-time PCR was performed with primers specific

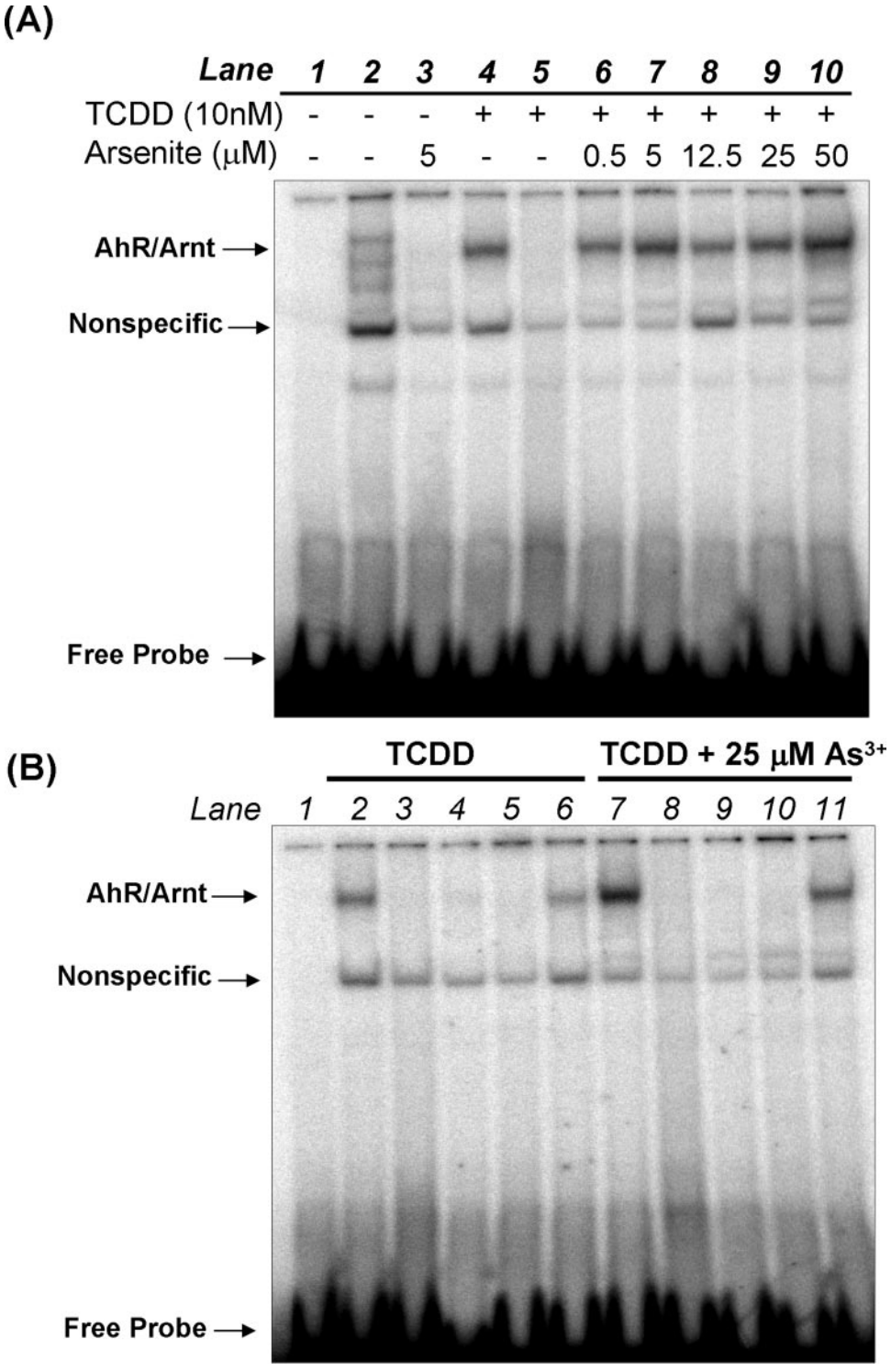

Fig. 5. Ah receptor nuclear translocation and DNA binding activity is unchanged by As^{3+} treatment. A, nuclear protein was prepared from HepG2 cells treated for 18 h with 10 nM TCDD and increasing concentrations of As^{3+} as described under *Materials and Methods*. Ten micrograms of nuclear protein was incubated with ^{32}P-XRE (5×10^5 cpm). Controls are as indicated: free probe (lane 1), DMSO treatment (lane 2), 5 μM As^{3+} treatment (lane 3), 10 nM TCDD treatment (lane 4), and TCDD treatment incubated with 200× unlabeled XRE as a specific competitor control (lane 5). Shifts of TCDD and As^{3+} cotreatments are indicated (lanes 6–10). Gel shown is representative of three independent shifts. B, supershift analysis was performed using 10 nM TCDD and 10 nM TCDD with 25 μM As^{3+} nuclear protein preparations. Activated AhR/Arnt binding complex was competed with 200× unlabeled XRE (lanes 2 and 7). Specificity of binding was determined by incubation with 200 ng of anti-Ah receptor (lanes 4 and 9) and 100 ng of anti-Arnt (lanes 5 and 10) antibodies. Nonspecific antibody binding was determined using excess anti-UGT (lanes 6 and 11).

MOL PHARM
MOLECULAR PHARMACOLOGY
aspet
Downloaded from molpharm.aspetjournals.org by guest on December 1, 2012

to the proximal promoter of *CYP1A1*. Because of the exponential nature of PCR, the C(t) value difference of 2 between DMSO- and TCDD-treated cells indicates an approximately 4-fold enrichment of promoter sequences detected in TCDD-treated cells (Fig. 6C). Cotreatment with 5 μM As^{3+} raised the C(t) value to almost basal levels, indicating a reduction in the amount of Pol II recruited to the promoter. These results suggest in conjunction with the hnRNA assay that As^{3+} inhibits the recruitment of the basic transcription machinery necessary for TCDD induction of CYP1A1.

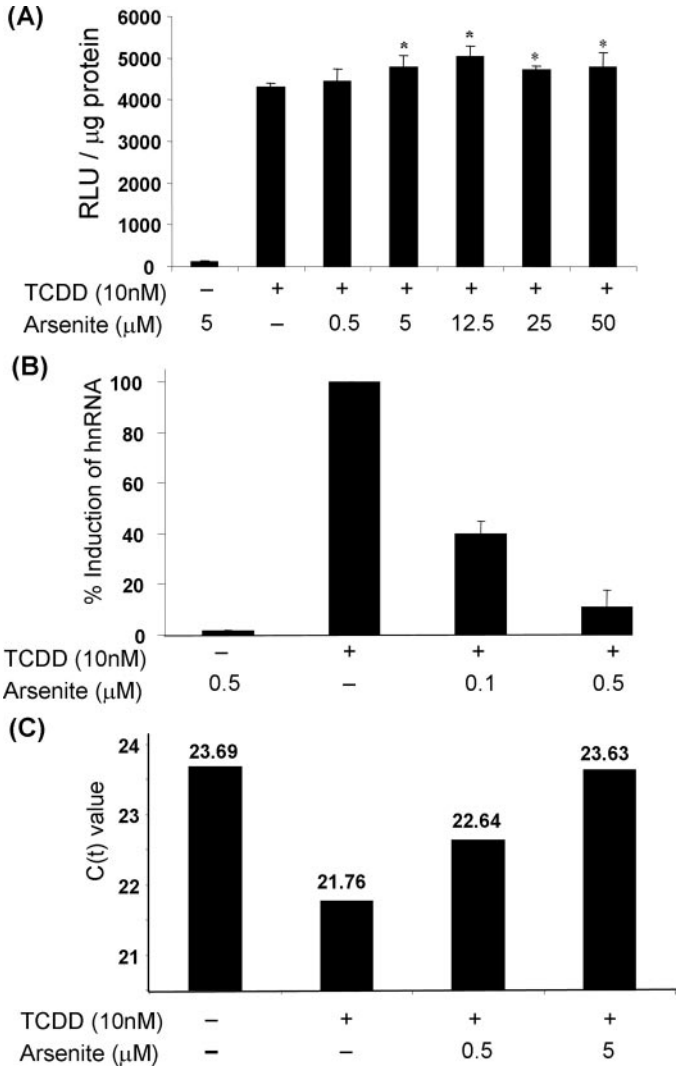

Fig. 6. Transcriptional control of CYP1A1. A, TV101L cells were cotreated for 18 h with 10 nM TCDD and increasing concentrations of As^{3+}. Results are displayed as RLU per microgram of cellular protein. All experiments were done in triplicate and a significant increase from 10 nM TCDD treatment is indicated (*, $P \leq 0.05$). B, HepG2 cells were treated for 1 h with TCDD or TCDD and As^{3+}. RNA was collected as described under *Materials and Methods*. Quantitative RT-PCR results using primers specific for CYP1A1 hnRNA were normalized to GAPDH and expressed as percentage of induction of TCDD-treated cells. C, chromatin immunoprecipitation assay was performed with HepG2 cells treated for 1 h with TCDD or TCDD and As^{3+}. Cells were cross-linked and incubated with antibody specific for Pol II. Recovered DNA was subjected to PCR with primers specific to the proximal promoter of *CYP1A1*. Results are shown as raw C(t) value and are representative of three independent pull-down experiments.

Discussion

Our results indicate that As^{3+}-initiated cell cycle arrest and the inhibition of CYP1A1 induction by TCDD are not associated with a common regulatory event. The disparity in these events can be observed by the very large differences in As^{3+} concentrations needed to induce G_2/M arrest and the inhibition of TCDD-initiated CYP1A1 induction. Very clear reductions in the induction of CYP1A1 mRNA and protein are observed at 0.5 μM As^{3+}, whereas the early events leading to G_2/M arrest are not detectable until 12.5 μM As^{3+} exposure. One may speculate that As^{3+} is capable of initiating cell cycle arrest at very low concentrations, but the sensitivity of detecting G_2/M arrest exceeds the limits of our techniques. Yet, when we analyzed the potential for cell arrest by monitoring changes in cell cycle regulatory proteins such as the cyclins B1 and D1 (Park et al., 2001; Zhao et al., 2002), p21, cdc25A, and cdk1 (Park et al., 2000), no observable changes in these proteins were detected with low concentrations of As^{3+} (data not shown). Furthermore, studies conducted in primary hepatocytes would question the role of cell cycle arrest in As^{3+} inhibition of TCDD-mediated CYP1A1 induction. Hepatocytes are quiescent cells in the intact liver but are capable of one to two progressions through the cell cycle during liver injury. In culture, primary hepatocytes progress through G_1 independent of stimulation but arrest in mid-G_1 after 42 h in culture (Loyer et al., 1996; Talarmin et al., 1999). The hepatocytes in our study were cultured for 48 h before treatment, allowing for cessation of cycling. Inhibition of TCDD-mediated CYP1A1 induction by As^{3+} was still observed and closely resembled the dose-response established in HepG2 cells. Thus, CYP1A1 induction was still dramatically inhibited in a quiescent cell model. These results demonstrate that the actions of As^{3+} on blocking CYP1A1 induction by TCDD are initiated through alterations in CYP1A1 transcription and are independent of the regulatory mechanisms initiated by As^{3+}-induced cell arrest.

The reduction in TCDD-induced CYP1A1-specific EROD activity by As^{3+} has been clearly established. Similar results have been observed when cells were cotreated with PAHs and As^{3+} (Jacobs et al., 1998, 1999; Vakharia et al., 2001; Vernhet et al., 2003). It has been postulated that this inhibition is the result of interference by As^{3+} with the catalytic potential of CYP1A1, either through reduction in cellular heme pools or by direct binding of As^{3+} to CYP1A1. However, changes in cellular heme pools would not lead to the changes in CYP1A1 transcription and the resulting reduction in CYP1A1 as determined by Western blot analysis.

The unique ability of As^{3+} to bind thiol groups is well established in vitro, whereas relevant cellular models of binding are more difficult to determine. As^{3+} has been shown to inhibit steroid binding to the glucocorticoid receptor (Simons et al., 1990; Stancato et al., 1993) and to inactivate the catalytic loop in IκB kinase β subunit, thereby reducing nuclear factor-κB activity (Kapahi et al., 2000). Members of the cytochromes P450 superfamily contain a conserved cysteine residue that serves as the axial ligand for heme iron (Johnson, 2003). However, P450s contain very few cysteine residues and in the crystal struc-

MOL PHARM
MOLECULAR PHARMACOLOGY
aspet
Downloaded from molpharm.aspetjournals.org by guest on December 1, 2012

MOL PHARM

MOLECULAR PHARMACOLOGY

ture of CYP2C5, no other cysteines are found in proximity to the heme binding cysteine. Because coupling to adjacent cysteine residues is a prerequisite for inhibition of protein function by As^{3+} and given the evidence presented here on down-regulation of CYP1A1 by a transcriptional mechanism, the inhibition of EROD activity is not the result of As^{3+} directly associating with CYP1A1.

Recent work has demonstrated a similar pattern of PAH-induced CYP1A1 inhibition by chromium (Wei et al., 2004). This work suggests that heavy metals may be acting in a similar manner at the promoter to inhibit induction of *CYP1A1.* However, chromium and As^{3+} show distinct patterns of gene expression alteration. As^{3+} alters the expression of a unique set of genes, most notably up-regulation of heme oxygenase 1, metallothionein, and NAD(P)H:quinone oxidoreductase, whereas chromium inhibits the expression of metallothionein and NQO1 (Maier et al., 2000; Andrew et al., 2003; Majumder et al., 2003; Zheng et al., 2003). Chromium's ability to cause DNA-protein cross-links has been suggested as a potential mechanism for HDAC1 sequestration on chromatin surrounding *CYP1A1,* a mechanism that has been proposed to inhibit CYP1A1 transcription. However, As^{3+}-induced cross-links and DNA damage have been repeatedly found using primarily very high cytotoxic concentrations (Yih and Lee, 2000; Mouron et al., 2001; Guillamet et al., 2004). Thus, it is doubtful that the low concentrations of As^{3+} used in our studies would impact on HDAC1 sequestration.

Our results suggest that the actions of As^{3+} leading to inhibition of CYP1A1 induction in HepG2 cells occur after TCDD-initiated activation of the Ah receptor and binding of the receptor to DNA. Because the nuclear concentrations of Ah receptor or the binding potential of the Ah receptor/Arnt complex to DNA is not compromised, the reductions in CYP1A1 hnRNA indicate that the rate of transcription initiated by TCDD may be slowed. Because of the low concentrations of As^{3+} needed to inhibit TCDD induction of CYP1A1, we would predict that As^{3+} is modifying essential regulatory proteins involved in the maintenance of polymerase-initiated transcription. In support of this, chromatin immunoprecipitation assays revealed a reduction in Pol II recruitment to the *CYP1A1* proximal promoter. Given the specificity of As^{3+} inhibition to CYP1A1, this suggests a block of a signaling event involved in the recruitment of Pol II to the gene.

Acknowledgments

We thank Dr. Fred Guengerich (Department of Biochemistry, Vanderbilt University) for a sample of the anti-CYP1A1 antibody and Dr. Christopher Bradfield for aliquots of the anti-Ah receptor and anti-Arnt antibodies.

References

Andrew AS, Warren AJ, Barchowsky A, Temple KA, Klei L, Soucy NV, O'Hara KA, and Hamilton JW (2003) Genomic and proteomic profiling of responses to toxic metals in human lung cells. *Environ Health Perspect* **111:**825–835.

Chen Y-H and Tukey RH (1996) Protein kinase C modulates regulation of the CYP1A1 gene by the Ah receptor. *J Biol Chem* **271:**26261–26266.

Chiou HY, Huang WI, Su CL, Chang SF, Hsu YH, and Chen CJ (1997) Dose-response relationship between prevalence of cerebrovascular disease and ingested inorganic arsenic. *Stroke* **28:**1717–1723.

Ciolino HP, Daschner PJ, Wang TT, and Yeh GC (1998) Effect of curcumin on the aryl hydrocarbon receptor and cytochrome P450 1A1 in MCF-7 human breast carcinoma cells. *Biochem Pharmacol* **56:**197–206.

Elferink CJ, Ge NL, and Levine A (2001) Maximal aryl hydrocarbon receptor activity depends on an interaction with the retinoblastoma protein. *Mol Pharmacol* **59:**664–673.

Filippova M and Duerksen-Hughes PJ (2003) Inorganic and dimethylated arsenic species induce cellular p53. *Chem Res Toxicol* **16:**423–431.

Galijatovic A, Beaton D, Nguyen N, Chen S, Bonzo J, Johnson R, Maeda S, Karin M, Guengerich FP, and Tukey RH (2004) The human *CYP1A1* gene is regulated in a developmental and tissue specific fashion in transgenic mice. *J Biol Chem* **279:**23969–23976.

Guillamet E, Creus A, Ponti J, Sabbioni E, Fortaner S, and Marcos R (2004) In vitro DNA damage by arsenic compounds in a human lymphoblastoid cell line (TK6) assessed by the alkaline Comet assay. *Mutagenesis* **19:**129–135.

Hestermann EV and Brown M (2003) Agonist and chemopreventative ligands induce differential transcriptional cofactor recruitment by aryl hydrocarbon receptor. *Mol Cell Biol* **23:**7920–7925.

Jacobs J, Roussel R, Roberts M, Marek D, Wood S, Walton H, Dwyer B, Sinclair P, and Sinclair J (1998) Effect of arsenite on induction of CYP1A and CYP2H in primary cultures of chick hepatocytes. *Toxicol Appl Pharmacol* **150:**376–382.

Jacobs JM, Nichols CE, Andrew AS, Marek DE, Wood SG, Sinclair PR, Wrighton SA, Kostrubsky VE, and Sinclair JF (1999) Effect of arsenite on induction of CYP1A, CYP2B and CYP3A in primary cultures of rat hepatocytes. *Toxicol Appl Pharmacol* **157:**51–59.

Johnson EF (2003) The 2002 Bernard B. Brodie award lecture: deciphering substrate recognition by drug-metabolizing cytochromes P450. *Drug Metab Dispos* **31:**1532–1540.

Kapahi P, Takahashi T, Natoli G, Adams SR, Chen Y, Tsien RY, and Karin M (2000) Inhibition of NF-κB activation by arsenite through reaction with a critical cysteine in the activation loop of IκB kinase. *J Biol Chem* **275:**36062–36066.

Lee MY, Jung BI, Chung SM, Bae ON, Lee JY, Park JD, Yang JS, Lee H, and Chung JH (2003) Arsenic-induced dysfunction in relaxation of blood vessels. *Environ Health Perspect* **111:**513–517.

Liu L, Trimarchi JR, Navarro P, Blasco MA, and Keefe DL (2003) Oxidative stress contributes to arsenic-induced telomere attrition, chromosome instability and apoptosis. *J Biol Chem* **278:**31998–32004.

Loyer P, Cariou S, Glaise D, Bilodeau M, Baffet G, and Guguen-Guillouzo C (1996) Growth factor dependence of progression through G_1 and S phases of adult rat hepatocytes in vitro. Evidence of a mitogen restriction point in mid-late G_1. *J Biol Chem* **271:**11484–11492.

Maier A, Dalton TP, and Puga A (2000) Disruption of dioxin-inducible phase I and phase II gene expression patterns by cadmium, chromium and arsenic. *Mol Carcinog* **28:**225–235.

Majumder S, Ghoshal K, Summers D, Bai S, Datta J, and Jacob ST (2003) Chromium(VI) down-regulates heavy metal-induced metallothionein gene transcription by modifying transactivation potential of the key transcription factor, metal-responsive transcription factor 1. *J Biol Chem* **278:**26216–26226.

Mosmann T (1983) Rapid colorimetric assay for cellular growth and survival: application to proliferation and cytotoxicity assays. *J Immunol Methods* **65:**55–63.

Mouron SA, Golijow CD, and Dulout FN (2001) DNA Damage by cadmium and arsenic salts assessed by the single cell gel electrophoresis assay. *Mutat Res* **498:**47–55.

Park JW, Choi YJ, Jang MA, Baek SH, Lim JH, Passaniti T, and Kwon TK (2001) Arsenic trioxide induces G_2/M growth arrest and apoptosis after caspase-3 activation and bcl-2 phosphorylation in promonocytic U937 cells. *Biochem Biophys Res Commun* **286:**726–734.

Park WH, Seol JG, Kim ES, Hyun JM, Jung CW, Lee CC, Kim BK, and Lee YY (2000) Arsenic trioxide-mediated growth inhibition in MC/CAR myeloma cells via cell cycle arrest in association with induction of cyclin-dependent kinase inhibitor, P21 and apoptosis. *Cancer Res* **60:**3065–3071.

Pfaffl MW (2001) A new mathematical model for relative quantification in real-time RT-PCR. *Nucleic Acids Res* **29:**e45.

Postlind H, Vu TP, Tukey RH, and Quattrochi LC (1993) Response of human *CYP1*-luciferase plasmids to 2,3,7,8-tetrachlorodibenzo-*p*-dioxin and polycyclic aromatic hydrocarbons. *Toxicol Appl Pharmacol* **118:**255–262.

Santini RP, Myrand S, Elferink C, and Reiners JJ Jr (2001) Regulation of Cyp1a1 induction by dioxin as a function of cell cycle phase. *J Pharmacol Exp Ther* **299:**718–728.

Schwerdtle T, Walter I, Mackiw I, and Hartwig A (2003) Induction of oxidative DNA damage by arsenite and its trivalent and pentavalent methylated metabolites in cultured human cells and isolated DNA. *Carcinogenesis* **24:**967–974.

Simons SS Jr, Chakraborti PK, and Cavanaugh AH (1990) Arsenite and cadmium(II) as probes of glucocorticoid receptor structure and function. *J Biol Chem* **265:**1938–1945.

Smith AH, Hopenhayn-Rich C, Bates MN, Goeden HM, Hertz-Picciotto I, Duggan HM, Wood R, Kosnett MJ, and Smith MT (1992) Cancer risks from arsenic in drinking water. *Environ Health Perspect* **97:**259–267.

Stancato LF, Hutchison KA, Chakraborti PK, Simons SS Jr, and Pratt WB (1993) Differential effects of the reversible thiol-reactive agents arsenite and methyl methanethiosulfonate on steroid binding by the glucocorticoid receptor. *Biochemistry* **32:**3729–3736.

Talarmin H, Rescan C, Cariou S, Glaise D, Zanninelli G, Bilodeau M, Loyer P, Guguen-Guillouzo C, and Baffet G (1999) The mitogen-activated protein kinase kinase/extracellular signal-regulated kinase cascade activation is a key signalling pathway involved in the regulation of G_1 phase progression in proliferating hepatocytes. *Mol Cell Biol* **19:**6003–6011.

Tchounwou PB, Patlolla AK, and Centeno JA (2003) Carcinogenic and systemic health effects associated with arsenic exposure–a critical review. *Toxicol Pathol* **31:**575–588.

Vakharia DD, Liu N, Pause R, Fasco M, Bessette E, Zhang QY, and Kaminsky LS (2001) Polycyclic aromatic hydrocarbon/metal mixtures: effect on PAH induction of CYP1A1 in human HepG2 Cells. *Drug Metab Dispos* **29:**999–1006.

Downloaded from molpharm.aspetjournals.org by guest on December 1, 2012

Vernhet L, Allain N, Le Vee M, Morel F, Guillouzo A, and Fardel O (2003) Blockage of multidrug resistance-associated proteins potentiates the inhibitory effects of arsenic trioxide on CYP1A1 induction by polycyclic aromatic hydrocarbons. *J Pharmacol Exp Ther* **304:**145–155.

Wei YD, Tepperman K, Huang MY, Sartor MA, and Puga A (2004) Chromium inhibits transcription from polycyclic aromatic hydrocarbon-inducible promoters by blocking the release of histone deacetylase and preventing the binding of p300 to chromatin. *J Biol Chem* **279:**4110–4119.

Yih LH and Lee TC (2000) Arsenite induces p53 accumulation through an ATM-dependent pathway in human fibroblasts. *Cancer Res* **60:**6346–6352.

Yueh MF, Huang YH, Hiller A, Chen S, Nguyen N, and Tukey RH (2003) Involvement of the xenobiotic response element (XRE) in Ah receptor-mediated induction of human UDP-glucuronosyltransferase 1A1. *J Biol Chem* **278:** 15001–15006.

Zhao S, Tsuchida T, Kawakami K, Shi C, and Kawamoto K (2002) Effect of As203 on cell cycle progression and cyclins D1 and B1 expression in two glioblastoma cell lines differing in p53 status. *Int J Oncol* **21:**49–55.

Zheng XH, Watts GS, Vaught S, and Gandolfi AJ (2003) Low-level arsenite induced gene expression in HEK293 cells. *Toxicology* **187:**39–48.

Address correspondence to: Dr. Robert H. Tukey, Leichtag Biomedical Research Bldg., Room 211, University of California, San Diego, La Jolla, CA 92093-0722. E-mail: rtukey@ucsd.edu

MOL PHARM

MOLECULAR PHARMACOLOGY

aspet

Downloaded from molpharm.aspetjournals.org by guest on December 1, 2012